Pergamon

0028-3908(95)00129-8

Neuropharmacology, Vol. 34, No. 11, pp. 1453–1467, 1995

0028-3908/95 $9.50 + 0.00

Detecting Changes in Calcium Influx Which Contribute to Synaptic Modulation in Mammalian Brain Slice

B. L. SABATINI and W. G. REGEHR*

Department of Neurobiology, Harvard Medical School, 220 Longwood Avenue, Boston, MA 02115, U.S.A.

(Accepted 10 August 1995)

Summary—The control of neurotransmitter release by modulation of presynaptic calcium influx was investigated at the granule cell to Purkinje cell synapse in rat cerebellar slices. Excitatory post-synaptic currents were measured using whole cell voltage clamp, and changes in presynaptic Ca influx were determined with the Ca-sensitive dye mag-fura-5. Single stimuli of the parallel fibers evoked rapid changes in mag-fura-5 fluorescence which increased from 10 to 90% in 1.4 msec, and then decayed within hundreds of milliseconds to prestimulus levels. These fluorescence changes were unaffected by disruption of internal stores with ryanodine or thapsigargin, and were reduced by 79% by the calcium channel toxin ω-conotoxin-MVIIC. We conclude that these signals result from calcium entry into presynaptic terminals through voltage gated calcium channels opened by action potentials. These fluorescence signals allow us to quantitate changes in calcium influx. We used this approach to study the enhancement of stimulus-evoked synaptic currents by 3-isobutyl-1-methylxanthine (IBMX), a phosphodiesterase inhibitor and antagonist of adenosine receptors. Both enhancement of calcium influx into presynaptic terminals, and reduction in the firing threshold of the parallel fibers, were found to contribute to IBMX-mediated synaptic enhancement. Changes in presynaptic calcium influx were also quantified with a novel method, which is unaffected by changes in fiber threshold. These studies illustrate some of the difficulties encountered when determining the factors responsible for synaptic enhancement and demonstrate how measurements of presynaptic calcium influx can contribute to our understanding of synaptic modulation. The approach described here promises to be widely useful in elucidating the role of calcium influx in the modulation of synapses in brain slice.

Keywords—Calcium channels, synaptic transmission, ω-conotoxin MVIIC, granule cells, Purkinje neuron, parallel fiber, 3-isobutyl-1-methylxanthine, thapsigargin, ryanodine.

Calcium entering presynaptic terminals through voltage gated calcium channels triggers neurotransmitter release (Katz and Miledi, 1967; Schweizer *et al.*, 1995). However, for many synapses it has been difficult to examine the role of calcium channels in synaptic transmission and to determine if changes in presynaptic calcium influx contribute to modulation of synaptic transmission. This has been the case for most synapses in the mammalian central nervous system, where presynaptic boutons are generally less than 1 μm in diameter and are therefore not amenable to eletrophysiological studies.

A key step in understanding how presynaptic calcium controls synaptic strength is to obtain a measure of calcium entering presynaptic terminals during action potentials (Delaney *et al.*, 1991). Previously a method was developed to selectively label fiber tracts in brain slices with fluorescent indicators (Regehr and Tank, 1991a). We have chosen to apply this method to the synapse between granule cells and Purkinje cells in the cerebellum for a number of reasons. By taking advantage of the architecture of the cerebellum (Palay and Chan-Palay, 1974), it is possible to obtain a region of the slice in which the only labeled structures are parallel fibers and their associated synaptic terminals. Furthermore, it is possible to obtain stable whole cell recordings from Purkinje cells and to voltage clamp synaptic currents evoked by parallel fiber activation (Llano *et al.*, 1991), thereby allowing us to directly correlate modifications of synaptic strength with changes in presynaptic calcium.

Here we extend previous studies on the role of presynaptic calcium in controlling the strength of synapses in the mammalian brain (Mintz *et al.*, 1995; Regehr and Atluri, 1995; Regehr *et al.*, 1994; Regehr and Tank, 1991a, b; Wu and Saggau, 1994a, b, c). We focus on the quantification of changes in presynaptic calcium influx for the synapse between cerebellar granule cells and Purkinje cells. We use a relatively new indicator,

*To whom correspondence should be addressed.

mag-fura-5 (Delbono and Stefani, 1993), for our calcium measurements, and find that it performs exceptionally well. Stimulus-evoked fluorescence changes in parallel fibers labeled with mag-fura-5 are shown to provide an accurate measure of the calcium entering presynaptic terminals through voltage gated calcium channels and to be independent of internal calcium stores. We use these fluorescence changes as a measure of calcium entry into presynaptic terminals, and examine the role of presynaptic calcium channels in the modulation of synaptic transmission. We examine the effects of 3-isobutyl-1-methylxanthine (IBMX), a phosphodiesterase inhibitor and antagonist of adenosine receptors (Smellie *et al.*, 1979). IBMX enhances synaptic transmission in the hippocampus (Chavez-Noriega and Stevens, 1994) and increases somatic calcium currents in cultured granule cells (Chavis *et al.*, 1994). We find that it has a number of complex presynaptic actions which include enhancing calcium influx into presynaptic terminals and lowering the firing threshold of the parallel fibers. These studies demonstrate how measurements of presynaptic calcium influx can be used to improve our understanding of synaptic modulation.

METHODS

Transverse slices (300 μm thick) were cut from the cerebellar vermis of 10–14 day old rats. In this orientation, the granule cell axons extend for several millimeters parallel to the surface of the slice in the molecular layer. Slices were allowed to recover for 1 hr at 32°C and then transferred to the recording chamber, where they were submerged in a volume of 1 ml and continuously superfused with oxygenated saline. Experiments were conducted at 20–24°C. The external solution (2 ml/min flow rate) consisted of (in mM): 125 NaCl, 2.5 KCl, 2 $CaCl_2$, 1 $MgCl_2$, 26 $NaHCO_3$, 1.25 NaH_2PO_4, and 25 glucose, 0.02 bicuculline, bubbled with 95% O_2 and 5% CO_2.

Ryanodine and thapsigargin were kept frozen as stock solutions in DMSO (100 mM and 10 mM, respectively). IBMX was dissolved in oxygenated external solution immediately prior to use.

Labeling procedure

Granule cell axons, known as parallel fibers, were labeled by local application of a solution containing the membrane permeant form of either mag-fura-5 (Delbono and Stefani, 1993) or fura-2 (Grynkiewicz *et al.*, 1985) (Molecular Probes, Eugene, OR), using a procedure described previously (Regehr and Atluri, 1995; Regehr and Tank, 1991a). Fifty μg of mag-fura-5 was dissolved in 20 μl of 25% Pluronic acid/75% DMSO, 300 μl of saline was added, and the solution was then vortexed for 1 min. Fast green was also included to facilitate visualization of the dye under bright field illumination. Loading with fura-2 was accomplished in the same manner, with the exception that the dye was diluted in 400 μl of saline. The loading time was 20 min for mag-fura-5 and 10 min for fura-2.

Measuring fluorescence levels

Experiments commenced 2–3 hr after loading. Parallel fiber tracts were stimulated extracellularly with a glass electrode (20–30 μm dia) placed in the molecular layer near the fill site. Fluorescence changes were measured in a 150 μm diameter spot 400–700 μm away from the stimulus site. An upright microscope (Zeiss Axioskop) and a 40× water immersion objective were used.

Illumination from a 150 W Xenon bulb was gated with a TTL pulse controlling an electromechanical shutter (Vincent Associates), and the area of illumination was defined by an iris diaphragm. The filter set used was 380 HT 15 excitation, a 430DCLP02 dichroic, and a 510WB40 emission filter (Omega Optical). The collected light was either focused onto a photodiode (Hamamatsu S1227-33BR) by a lens located in the image plane, or was collected with a photomultiplier tube (Hamamatsu HC124-06MOD). Calcium increases produce a decrease in fluorescence for the dyes used in these studies with 380 nm excitation. All fluorescence traces in this paper have been inverted for display.

Fura saturation studies

Changes in fluorescence levels using 380 nm excitation were recorded following 100 Hz trains of 1–4 stimuli. In order to monitor resting calcium levels, basal fluorescence levels under 340 and 380 nm wavelength excitation were measured and their ratio monitored. Each stimulus series consisted of 6 repetitions of 1 and 2 action potentials and 1 each of 3 and 4 action potential trains. The entire series, including 2 sets of measurements of resting fluorescence levels, was completed in 12 min and repeated without interruption throughout the course of the experiment.

Fluorescence images

The fluorescence images of Fig. 1 were acquired with a cooled, charge-coupled device camera (Photometrics). Low power images were obtained using a 10× water immersion objective and a 0.55× projection lens. Images were recorded with a Macintosh Centris 650 computer running IPLab software (Signal Analytics, Vienna, VA).

Extracellular field recordings

Extracellular potential recordings were made with 2.0–3.0 MΩ glass pipettes filled with external solution and placed near the surface of the parallel fibers 400–700 μm from the stimulating electrode. In experiments in which fluorescence level measurements and field recordings were made simultaneously, the recording pipette was placed at the edge of the spot of fluorescence illumination at the same approximate depth as the labeled fibers. Field potentials were amplified 100× with an Axon Instru-

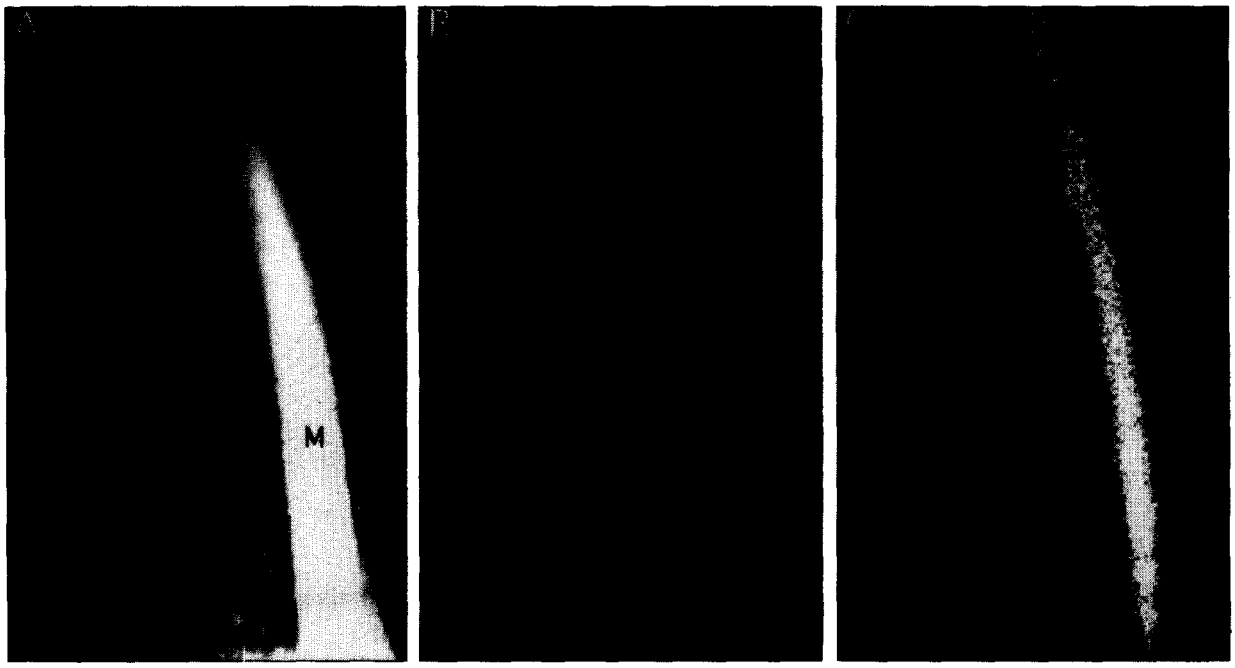

Fig. 1. Mag-fura-5 labeling and spatial extent of parallel fiber activation. (A) Fluorescence image of mag-fura-5 labeling. Molecular, Purkinje cell, and granular layers are labeled M, P and G respectively. Changes in mag-fura-5 fluorescence resulting from a stimulus train of low (B) and high (C) stimulus strength. Relative $\Delta F/F$ signals are shown in gray scale with white corresponding to large increases in cytosolic calcium (a 3% decrease in $\Delta F/F$), and black to no change in calcium levels. Trains consisted of 20 stimuli commencing at the beginning of a 300 msec exposure. B and C are the average of four images. Image size is 750 μm by 1300 μm.

ments Axopatch 200 A in current clamp mode and were filtered at 10 KHz.

Measuring synaptic currents

Whole cell recordings of Purkinje neurons were obtained as previously described (Regehr and Mintz, 1994), using 1.7–2.5 MΩ glass pipettes containing an internal solution of (in mM): 35 CsF, 100 CsCl, 10 EGTA, 10 KHEPES, 0.1 D600, pH = 7.3 with CsOH. The access resistance (< 5 MΩ after series resistance compensation) and leak current (0 to −100 pA) were continuously monitored. If either of these quantities changed, the experiment was terminated, and data was not included for analysis.

Parallel fibers were stimulated extracellularly with a bipolar electrode placed in the molecular layer several hundred microns from the recording electrode. The resulting EPSC decayed with a time constant of 5–7.5 msec and the time course of decay remained constant throughout each experiment. Low stimulus intensities were used to keep synaptic currents small and the resulting voltage errors arising from uncompensated series resistance below 4 mV.

Data acquisition and analysis

Outputs of the photodiode, photomultiplier tube and Axopatch 200 A were recorded digitally with a 16-bit D/A converter (Instrutech, Great Neck, NY), pulse control software (Herrington and Bookman, 1994) and a Apple Macintosh Centris 650 computer. Analysis was done on-and off-line with Igor Pro software (Wavemetrics, Lake Oswego, OR).

RESULTS

Detection of calcium transients in parallel fiber presynaptic terminals

In previous studies, we found that several low affinity dyes, such as furaptra (Raju *et al.*, 1989), were well suited to detecting the rapid calcium transients in cerebellar granule cell presynaptic terminals (Regehr and Tank, 1992). Here we test another indicator, mag-fura-5, to see if it offers any advantages.

An example of the labeling obtained with mag-fura-5 is shown in Fig. 1(A). The loading site was in the molecular layer (M) just below the band of intensely labeled parallel fibers. To the left of the band of parallel fibers lies the Purkinje cell layer (P), which contains the unlabeled cell bodies of Purkinje cells. Further to the left lies the granular layer (G), which contains backfilled granule cell bodies. Figure 1(B) illustrates the spatial extent of fiber activation with an electrode placed in the molecular layer. The light band corresponds to a region in which the fluorescence levels changed significantly upon stimulation. As shown in Fig. 1(C), a wider band of fibers was activated with a higher stimulus intensity. The absence of fluorescence changes in the granular layer indicates that calcium transients in the cell bodies of the

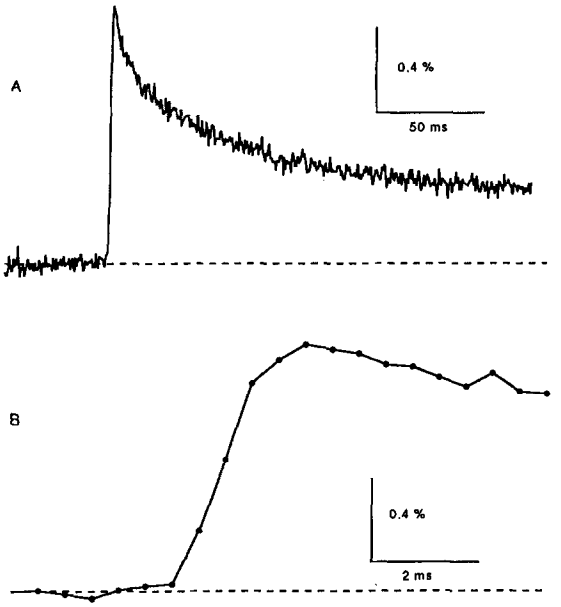

Fig. 2. High temporal resolution measurements of mag-fura-5 fluorescence changes evoked by single stimuli. A and B are the average of 80 trials and are the same trace plotted with different time scales.

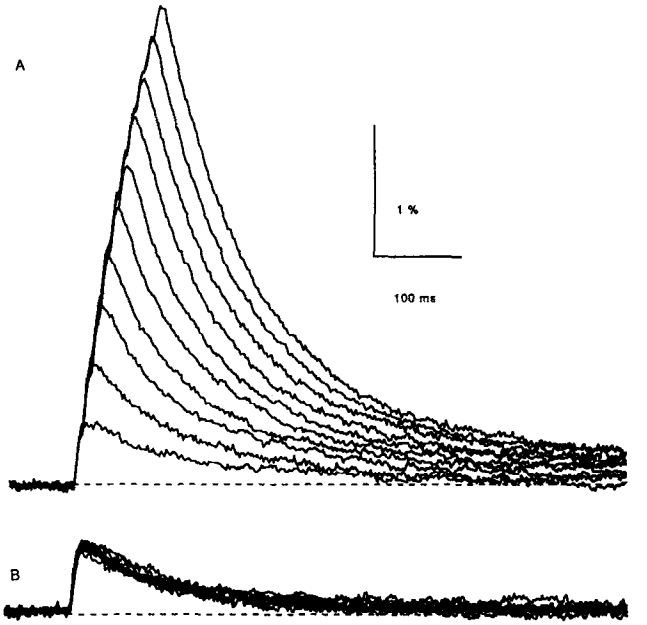

Fig. 3. Changes in mag-fura-5 fluorescence during brief stimulus trains. (A) Fluorescence transients produced by 100 Hz trains of 1–10 stimuli. (B) Fluorescence increases caused by each additional stimulus. Traces were determined by subtracting transients produced by n stimuli from those produced by n+1 stimuli in (A), and shifting the x-axis to align the peaks. Traces are averages of three trials.

granule cells are not sufficiently large to be detected for these experimental conditions.

Experiments were conducted to measure the time course of calcium transients (Fig. 2). Fluorescence was collected from a spot hundreds of microns from the stimulus electrode (2 kHz filtering). The fluorescence signal rose extremely rapidly [Fig. 2(B)], with an average 10–90% rise time of 1.38 ± 0.05 msec (n = 5, ± SEM).

The return of fluorescence to resting levels can be crudely approximated by an exponential decay with a time constant of 90–150 msec, but it is better fit by a double exponential. This decay time is similar to that reported previously (Regehr and Atluri, 1995) for other low affinity indicators, such as furaptra and BTC (Iatridou *et al.*, 1994).

In order to quantitate changes in calcium influx, it is important to establish that the relationship between calcium influx and fluorescence changes is linear. Figure 3(A) shows mag-fura-5 fluorescence transients evoked by a series of stimulus trains consisting of 1–10 stimuli. In these experiments the signal was filtered at 200 Hz to improve the signal-to-noise ratio. As shown in Fig. 3(B), each stimulus pulse in the train produces the same incremental increase in calcium. As found for other low affinity dyes, mag-fura-5 responds linearly to calcium increases over the range of calcium concentrations in these experiments, in contrast to high affinity dyes such as fura-2 (Regehr and Atluri, 1995).

The contribution of internal calcium stores to calcium transients in presynaptic terminals

Experiments were performed to determine if internal stores contribute to fluorescence signals, as is known to occur in Purkinje cell dendrites (Llano *et al.*, 1994), hippocampal pyramidal cells (Alford *et al.*, 1993), and the somata of cultured granule cells (Irving *et al.*, 1992). We tested the effects of two compounds known to affect internal stores, ryanodine and thapsigargin. In these experiments, a band of parallel fibers was labeled in the usual way, and we determined the effects of these agents on fluorescence transients produced by single stimuli. Both of these compounds have previously been used with success in brain slices (Alford *et al.*, 1993; Llano *et al.*, 1994). Ryanodine is known to interact with an intracellular channel which is typically opened by calcium, and which is responsible for calcium-induced calcium release (Feher and Lipford, 1985; Rousseau *et al.*, 1987). Thapsigargin affects the calcium ATPase responsible for loading internal stores (Lytton *et al.*, 1991; Sagara and Inesi, 1991). As shown in representative experiments, prolonged applications of 20 μM ryanodine [Fig. 4(A)] or 10 μM thapsigargin [Fig. 4(B)] did not affect the peak values of fluorescence transients. The average peak fluorescence values were 101.3 ± 3.3% of control values (n = 3, ± SEM) for ryanodine and 103.3 ± 2.6% (n = 3, ± SEM) for thapsigargin.

Contribution of voltage gated calcium channels to presynaptic calcium transients

We tested the sensitivity of the fluorescence transients to the peptide toxin ω-conotoxin-MVIIC (Hillyard *et al.*, 1992) (Fig. 5). This toxin has been shown to block a large fraction of calcium current in central neurons by affecting

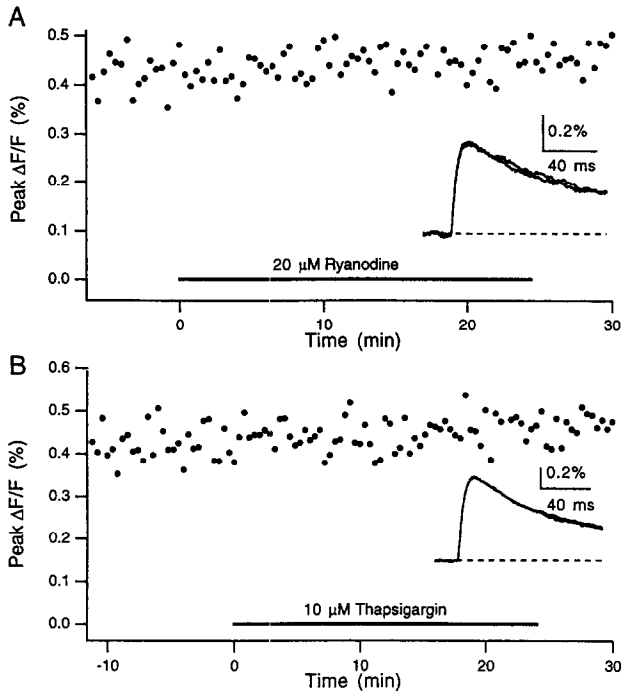

Fig. 4. Disruption of internal stores does not affect mag-fura-5 fluorescence transients. The effect of ryanodine (A), and thapsigargin (B), on peak changes in mag-fura-5 fluorescence produced by single stimuli. Insets show average fluorescence transients in control conditions and after the application of thapsigargin or ryanodine.

several calcium current components. We found that ω-conotoxin-MVIIC (1.5 μM) reduced stimulus evoked fluorescence transients by 79 ± 2% ($n = 3$, ± SEM). This provides strong evidence that the fluorescence transients we detect are produced by calcium influx through voltage gated calcium channels.

Testing the contribution of changes in calcium entry to modulations of synaptic strength

Taken together the experiments of Figs 2–5 provide evidence that we can obtain an accurate measure of calcium increases in presynaptic terminals. As dealt with at length in the Discussion, this provides us with a means of detecting changes in presynaptic calcium influx. We will next demonstrate the use of this optical approach to test for the involvement of changes in calcium entry in synaptic modulation.

We set out to test the actions of IBMX on synaptic transmission at the parallel fiber to Purkinje cell synapse. IBMX (50 μM) enhanced the amplitude of stimulus-evoked synaptic currents by 230 ± 60% ($n = 6$, ± SD, range 184–354%), and by 232% in the representative experiment of Fig. 6. There was substantial variability in the degree of enhancement.

The synaptic enhancement in the presence of IBMX could come from a variety of sources, including changes in fiber threshold, changes in presynaptic calcium influx,

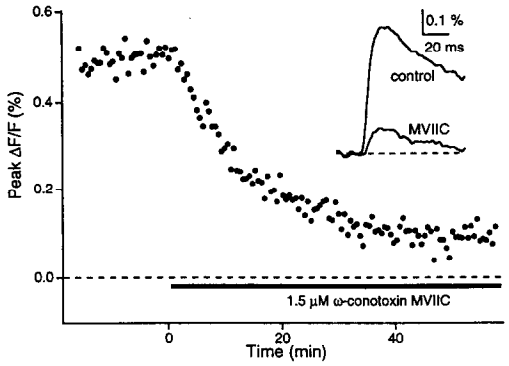

Fig. 5. Mag-fura-5 fluorescence transients evoked by a single stimulus of the parallel fibers are greatly attenuated by the calcium channel toxin ω-conotoxin-MVIIC. Inset shows average traces before application of the toxin and after block had reached steady state.

presynaptic changes downstream from calcium, or postsynaptic changes.

We tested the effect of IBMX on the number of fibers stimulated (Fig. 7). Parallel fibers were stimulated with an electrode placed in the molecular layer, and the resulting extracellular field potentials were recorded in the molecular layer well away from the stimulus electrode. Stimulation produced a well-characterized extracellular signal, which corresponds to the extracellular current flow accompanying a propagating action potential in the parallel fibers (Eccles *et al.*, 1967). The amplitude of this response provides a sensitive measure of the number of parallel fibers activated.

IBMX affects the presynaptic volley by changing the time to peak and increasing its amplitude [Fig. 7(Aa)]. A comparison of the wave forms obtained in IBMX with those obtained in control conditions reveals no additional changes in the presynaptic waveform [Fig. 7(Ab)]. The shift in the time to peak appears to be a consequence of an increase in the conduction velocity. The increase in the amplitude of the presynaptic volley reflects a change in the number of parallel fibers activated. As shown in

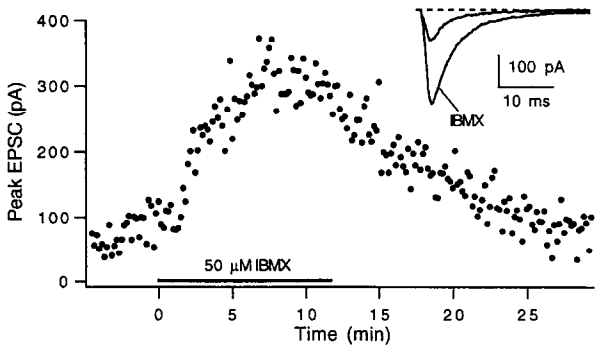

Fig. 6. IBMX enhances evoked synaptic currents. Inset shows synaptic currents in control conditions and after the effects of IBMX had plateaued.

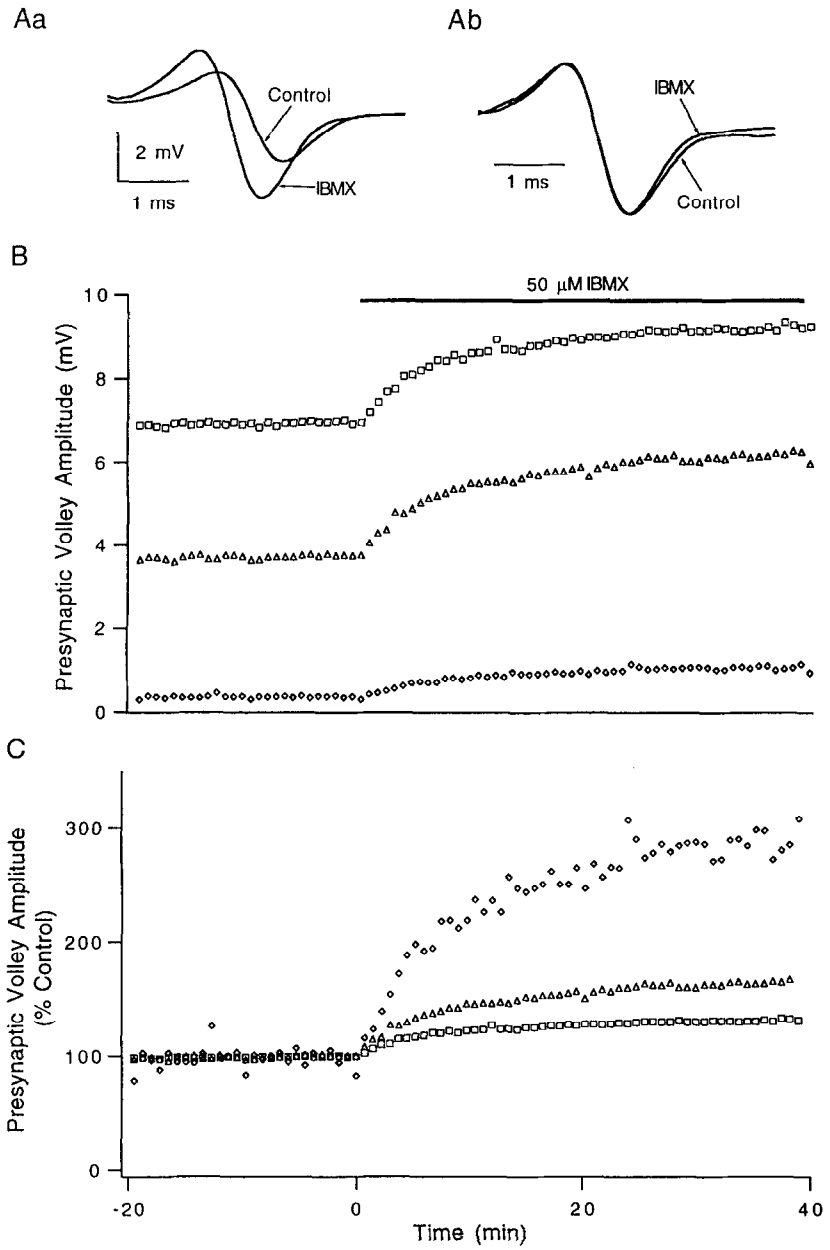

Fig. 7. IBMX affects the threshold for parallel fiber activation. (Aa) Presynaptic volley in control conditions and after the effects of IBMX had reached steady state. (Ab) The same traces as in (Aa) with normalized amplitudes. The presynaptic volley in control conditions has been scaled by a factor of 1.7 and shifted by 300 μsec. (B) The presynaptic volley amplitude is plotted as a function of time before and after the application of IBMX. Different symbols correspond to stimulus pulse durations of 0.8 msec (squares), 0.5 msec (triangles), and 0.2 msec (diamonds). (C) The presynaptic volley amplitudes have been normalized relative to control values for the three different stimulus strengths. The presynaptic volleys of (A) correspond to the amplitudes denoted by the triangles in (B) and (C); they are the average of 10 trials.

Fig. 7(C), this increase was more pronounced when a small number of fibers were stimulated: expressed as percent increase relative to control levels, the enhancement of extracellular fields for the smallest stimulus strength was 187%, and was just 31% for the largest stimulus strength.

We next sought to determine if increases in presynaptic calcium influx also contribute to the enhancement produced by IBMX. In attempting to detect changes in calcium influx, it is important to take into account increases in the number of fibers activated in the presence of IBMX. We simultaneously measured the effect of IBMX on mag-fura-5 $\Delta F/F$ signals [Fig. 8(A)] and on the presynaptic volley [Fig. 8(B)]. Since the amplitude of fluorescence transients scales as the number of fibers stimulated, we corrected for changes in fiber activation to obtain a measure of the average change in calcium influx per fiber stimulated [Fig. 8(C)]. We found that IBMX enhanced calcium influx by 24% in this experiment, and

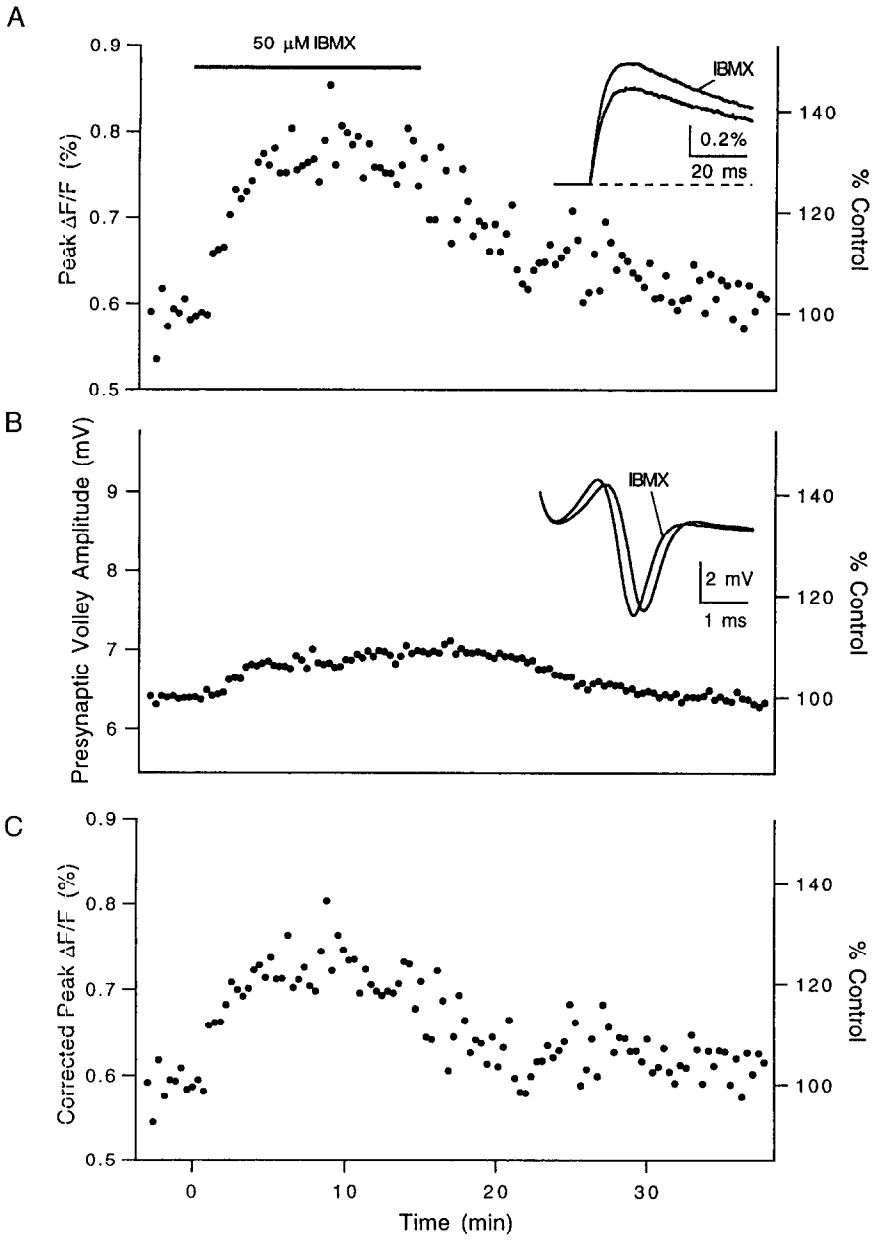

Fig. 8. Mag-fura-5 fluorescence measurements reveal that IBMX enhances calcium influx into parallel fiber presynaptic terminals. The effect of IBMX on mag-fura-5 fluorescence transients produced by single stimuli (A), on the presynaptic volley amplitude (B), and on the mag-fura-5 transients corrected for changes in the number of fibers stimulated (C).

on average by 30 ± 8% ($n = 4$ from 2 slices, ± SD, range 20–38%).

We tested the possibility that IBMX affects resting calcium levels. We found that in unstimulated parallel fibers labeled with the high affinity dye fura-2, the fluorescence ratio for 340 and 380 nm illumination was unchanged by IBMX ($n = 3$, data not shown), indicating that resting calcium levels remained constant.

We also determined the magnitude of changes in calcium influx with a method which is insensitive to the number of activated fibers. This method detects changes in calcium influx from the extent of saturation of high affinity dyes such as fura-2, and is described in detail in the Appendix. Changes in fluorescence transients for one and two stimuli are shown in Fig. 9. In the presence of IBMX the magnitudes of these fluorescence transients increases [Fig. 9(A,B)]. It is not straightforward to use this increase in amplitude to determine the change in size of the calcium transients because: (1) as for mag-fura-5, the magnitude of these changes scales as the number of fibers activated, and (2) as described previously calcium changes in parallel fibers are sufficiently large to begin to saturate high affinity calcium indicators such as fura-2 (Regehr and Atluri, 1995). However, it is possible to

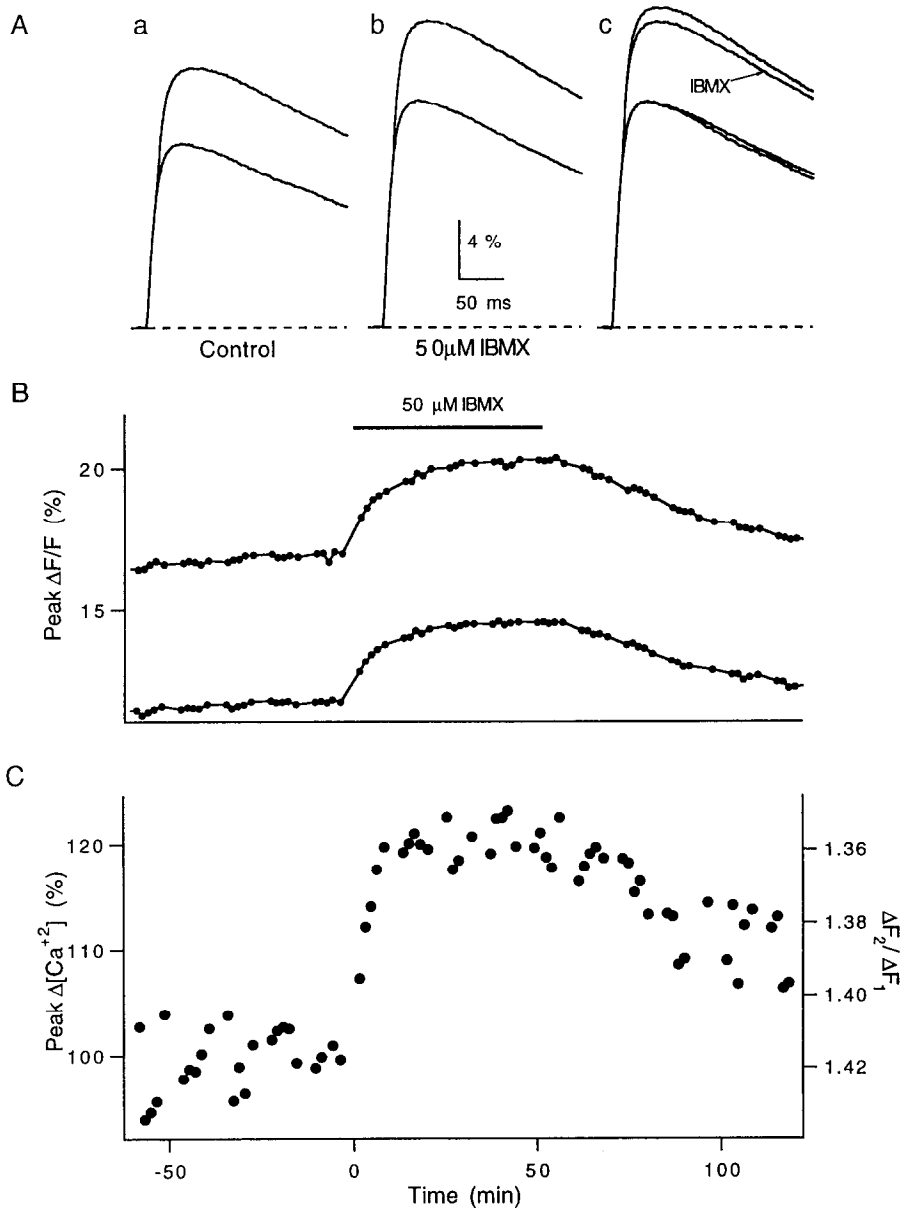

Fig. 9. Fura-2 fluorescence measurements reveal that IBMX enhances calcium influx into parallel fiber presynaptic terminals. Fluorescence changes produced by 1 stimulus and by 2 stimuli separated by 10 msec in control conditions (Aa) and in the presence of IBMX (Ab). In (Ac) the control traces have been scaled by a factor of 1.2 to show the effect of IBMX on the relative sizes of fluorescence changes produced by 2 and 1 stimuli. (B) The effect of IBMX as a function of time on peak $\Delta F/F$ signals produced by one and two stimuli. (C) The effect of IBMX on relative calcium influx determined from the change in the ratio of the peaks of the fluorescence transients produced by 2 and 1 stimuli.

determine changes in calcium influx from the relative sizes of fluorescence changes produced by 2 and 1 stimuli [Fig. 9(Ac,C)]. Using this approach we find that IBMX increases calcium influx by 22.4 ± 2.0% ($n = 3$, ± SD).

DISCUSSION

Detecting calcium transients in parallel fibers with mag-fura-5

Mag-fura-5 compares favorably to other indicators we have used to detect presynaptic transients. Mag-fura-5 labeled fiber tracts very well, gave slightly larger fluorescence changes than furaptra (consistent with its dissociation constant for Ca of 23 μM compared to 49 μM for furaptra (Delbono and Stefani, 1993)), and responded linearly to calcium changes. Even though mag-fura-5 is quite sensitive to changes in magnesium (a dissociation constant for Mg of 0.5 mM compared to 5 mM for furaptra (Delbono and Stefani, 1993)), this did not appear to interfere with the use of this dye in

detecting calcium transients. These properties make mag-fura-5 a leading choice for experiments in which calcium influx is to be quantified.

Fluorescence transients are due to calcium entry through voltage gated calcium channels

A number of lines of evidence suggest that the observed fluorescence changes are a consequence of calcium influx through voltage gated calcium channels: the signals are largely attenuated by calcium channel antagonists, are not affected by disruption of internal stores, and have short rise times.

The observation that ω-conotoxin-MVIIC reduced fluorescence transients by 79% demonstrates that this signal results largely from calcium entry through voltage gated calcium channels. This toxin blocks multiple components of calcium current (Hillyard *et al.*, 1992). However, there is a component of calcium current which is insensitive to ω-conotoxin-MVIIC in somatic recordings from cultured granule cells (Randall and Tsien, 1995); thus the remaining 21% of the fluorescence signal may well be due to calcium entry through calcium channels resistant to ω-conotoxin-MVIIC. The effect of ω-conotoxin-MVIIC builds upon previous studies (Mintz *et al.*, 1995; Regehr and Atluri, 1995), which have shown that fluorescence transients are reduced by Cd in a dose-dependent manner with a K_d of 6 μM, they are attenuated in low external calcium, and they are reduced in an additive manner by ω-Aga-IVA (Mintz *et al.*, 1992a; Mintz *et al.*, 1992b) and ω-conotoxin (Fujita *et al.*, 1993; Williams *et al.*, 1992), which lower $\Delta F/F$ signals by 50 and 27% respectively.

We also found that thapsigargin and ryanodine, which disrupt internal stores of calcium and affect calcium induced calcium release, did not change peak calcium levels. It appears that stores targeted by these agents have a much larger role in dendritic and somatic signaling (Alford *et al.*, 1993; Irving *et al.*, 1992; Llano *et al.*, 1994) than in presynaptic terminals; this is consistent with the observed antibody localization of the ryanodine receptor and the vacuolar calcium-ATPase (Ellisman *et al.*, 1990; Kuwajima *et al.*, 1992; Sharp *et al.*, 1993; Takei *et al.*, 1992).

The 10–90% rise time of fluorescence transients is about 1.4 msec. This is consistent with the predicted time course of calcium current resulting from depolarization by an action potential, since increases in cytoplasmic calcium can be thought of as the integral of the calcium current.

Previously we have shown that the fluorescence transients are eliminated by TTX (Regehr and Atluri, 1995), suggesting that an action potential is required. In addition the fluorescence transients do not have post synaptic contributions (they are unaffected by CNQX (Honore *et al.*, 1988) which completely blocks synaptic currents at the granule cell to Purkinje cell synapse (Konnerth *et al.*, 1990)).

Taken together, these findings indicate that the fluorescence transients we observe result from calcium entry through voltage gated calcium channels opened by action potentials. It is likely that most of the signal is from presynaptic boutons which make up an estimated 75% of the volume of parallel fibers (Palay and Chan-Palay, 1974). Furthermore, calcium channels are typically present in presynaptic terminals at much higher densities than in axons (Cohen *et al.*, 1991; Robitaille and Charlton, 1992; Smith *et al.*, 1993). Since parallel fibers make the vast majority of their synaptic contacts with Purkinje cells (Palkovits *et al.*, 1971), we conclude that these fluorescence transients arise from boutons associated with the granule cell to Purkinje cell synapse.

Optical detection of changes in calcium influx

In the previous section, we established that the changes in mag-fura-5 fluorescence are produced by calcium influx through voltage gated calcium channels. These signals can be used to detect changes in calcium influx into presynaptic terminals (Regehr and Atluri, 1995). We have shown that for a train of stimuli the incremental increase in fluorescence remains constant. The most straightforward interpretation of this observation is that each stimulus increases free calcium by the same amount and that the peak change ΔF/F of mag-fura-5 is linearly related to the total calcium current entering during an action potential,

$$\left(\frac{\Delta F}{F}\right)_{peak} \propto \mathrm{Ca}_{\mathrm{influx}} = \int \mathrm{I}_{\mathrm{Ca}}\mathrm{d}t. \qquad (1)$$

Thus, a change in calcium influx per spike will produce the same change in the $\Delta F/F$ signal, provided the number of fibers activated remains constant.

It is also helpful to consider the factors controlling calcium dynamics in presynaptic terminals. A quantitative description of calcium dynamics has been developed from studies on chromaffin cells (Neher and Augustine, 1992) and crayfish presynaptic terminals (Tank *et al.*, 1995) [Fig. 10(A)]. When calcium enters a presynaptic terminal it binds to calcium buffers, and is then removed from the cytoplasm, either to internal stores or to the cell exterior. For low affinity calcium indicators, such as mag-fura-5,

$$\left(\frac{\Delta F}{F}\right)_{peak} \propto \Delta[\mathrm{Ca}]_i \propto \left(\frac{[\mathrm{B}]}{K_B} + \frac{[F]}{K_F}\right)^{-1} \mathrm{Ca}_{\mathrm{influx}}, \qquad (2)$$

where [B] and K_B are the concentration and the dissociation constant of the endogenous buffer, and $[F]$ and K_F are the concentration and the dissociation constant of the calcium indicator. This relationship applies when $[\mathrm{Ca}]_i << K_B$ and $[\mathrm{Ca}]_i << K_F$, and that the indicators and endogenous buffers are in equilibium with the calcium. The decay of calcium is approximated by

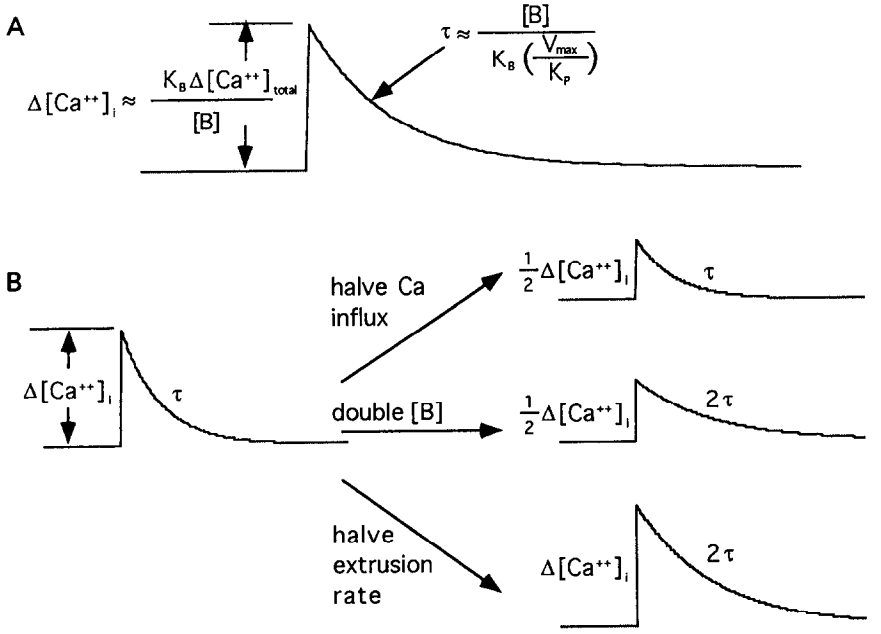

Fig. 10. Effects of changes in calcium influx, buffering and extrusion on calcium accumulation. (A) Simplified view of calcium dynamics in presynaptic terminals. (B) Effects of changing calcium influx, buffer concentration, or extrusion rate on the calcium dynamics.

$\tau = ([B]/K_B)(V_{max}/K_p)^{-1}$, where V_{max}/K_p is proportional to the rate of calcium extrusion from the cytoplasm.

Figure 10(A) and Eq. (2) bear directly on the interpretation of our experiments: changing influx, extrusion or buffer capacity can all affect calcium transients. Altering influx affects peak $\Delta F/F$ but not the time course of calcium decay. Changing buffer capacity affects both the time course of calcium decay and peak $\Delta F/F$. Modifying the extrusion rate changes the time course of calcium decay without affecting peak $\Delta F/F$. Thus, it is possible to distinguish experimentally between changes in influx, buffering and extrusion [Fig. 10(B)].

Calcium channel modulation contributes to enhancement of synaptic strength by IBMX

IBMX enhanced stimulus-evoked synaptic currents by an average of 232%. Using two different techniques we found that IBMX also increased calcium influx. From changes in mag-fura-5 $\Delta F/F$ signals (corrected for the number of fibers stimulated) we estimate that calcium influx is enhanced by 30%. Using a method that is insensitive to the number of fibers activated (Appendix), we found that calcium influx is enhanced by 22%.

To estimate the extent to which calcium influx contributes to synaptic enhancement, it is necessary to know the relationship between calcium influx and release. In previous studies (Mintz *et al.*, 1995) we found that when calcium influx is altered by changing external calcium, or by blocking calcium channels with Cd or ω-conotoxin-GVIA, the relationship between EPSC amplitude and calcium influx can be approximated by an expression of the form

$$(\text{EPSC amplitude}) \propto (\text{Ca}_{\text{influx}})^n, \qquad (3)$$

where $n \sim 2.5$. According to Eq. (3), and assuming that $n = 2.5$, we predict that the increase in calcium influx we observe accounts for a synaptic enhancement of 64–92%. We have also found that channels sensitive to ω-Aga-IVA appear to be more effective than other types of calcium channels at triggering the release of neurotransmitter (Mintz *et al.*, 1995); we estimate that $n = 4$ for release mediated by these channels. We predict that if ω-Aga-IVA-sensitive channels are selectively modulated, the increase in calcium entry we observe accounts for a synaptic enhancement of 121–185% [Eq. (3) with $n = 4$].

Although it is clear that IBMX increases presynaptic calcium influx, further studies, as described below, are needed to refine our estimates of the contributions of changes in calcium entry to IBMX-mediated synaptic enhancement.

Effects of IBMX on fiber excitability and conduction velocity

IBMX affected the presynaptic volley in two ways (Fig. 7). First, the same stimulus activated more fibers in the presence of IBMX; it appears that IBMX lowers the threshold for extracellular stimulation. This effect is more pronounced for small stimulus intensities, perhaps because more fibers are near threshold. Second, application of IBMX increased the conduction velocity of the parallel fiber, which shifted the presynaptic volley by 200–300 μsec. Although further studies are required to

elucidate the mechanisms responsible for these effects, they could both be caused by modulating either leak potassium channels, or sodium channels involved in spike initiation.

It is interesting to speculate on the physiological significance of the changes in conduction velocity and fiber excitability produced by IBMX. Although the threshold effects we observed were on extracellular stimulation, it is possible that a similar threshold effect occurs for spike initiation in the initial segment of the granule cell. The effect of IBMX on the conduction velocity suggests that there is a mechanism to alter parallel fiber conduction velocity which could control the timing of signals between granule cells and Purkinje cells.

General issues regarding the determination of the role of changes in calcium influx in modulation of synaptic transmission

The approach taken here for IBMX is intended as a demonstration of the manner in which optical detection of calcium influx will facilitate the investigation of the role of calcium influx in synaptic modifications. The first step in determining the extent to which calcium entry contributes to synaptic modulation is to quantify the fractional change in calcium entry. In most of our studies we have quantified changes in calcium entry by using low affinity indicators and measuring the effects of modulators on the $\Delta F/F$ signals evoked by single stimuli. As discussed in detail elsewhere (Mintz *et al.*, 1995; Regehr and Atluri, 1995) there are a number of precautions which should be taken when quantifying calcium influx with this approach: (i) care should be taken in the labeling process to avoid labeling structures other than the ones of interest; (ii) it should also be verified that $\Delta F/F$ signals are obtained only from presynaptic structures; (iii) the ratio method is not applicable and should not be used; (iv) high affinity calcium indicators should not be used, to avoid saturation of responses and distortion of the signals (Feller *et al.*, 1995; Regehr and Atluri, 1995); (v) care should be taken not to alter the calcium dynamics in the presynaptic terminal by introducing an excess of calcium indicator; (vi) it is crucial that the steady state conditions are reached (this can take a surprisingly long time in brain slice); (vii) changes in the numbers of fibers excited must be taken into account (as was done here for IBMX).

A more complete examination of the involvement of changes of calcium influx in synaptic modulation is provided elsewhere for the granule cell to Purkinje cell synapse by adenosine or baclofen (Dittman and Regehr, in preparation). In that study a number of additional steps are taken: (i) a dose response curve is obtained for both synaptic transmission and calcium influx, (ii) the pharmacological sensitivity of the channels being modulated is examined, (iii) effects of modulators on miniature post synaptic currents are determined to test for presynaptic modulation of release downstream from calcium influx, and (iv) the curve relating calcium influx and release for the modulator being tested are compared to similar curves obtained when calcium entry was manipulated in ways known to affect influx through calcium channels.

APPENDIX: DETECTION OF CHANGES IN PRESYNAPTIC CALCIUM INFLUX USING THE SATURATION OF HIGH AFFINITY INDICATORS

In this section we introduce a method for detecting changes in presynaptic calcium influx. This approach offers the advantage that it is insensitive to changes in the number of fibers activated.

As has been described previously, the increases in bulk calcium which accompany single stimuli are sufficient to begin to saturate high affinity indicators such as fura-2. This leads to a decrease in the fluorescence change per stimulus for successive stimuli in a train, even though the influx per stimulus remained constant. Previously, we used the degree of saturation of fura-2 during a stimulus train to quantify the calcium influx during a spike (about 200 nM, for a fura-2 dissociation constant of 200 nM and resting calcium of 50 nM; Regehr and Atluri, 1995).

We also found that during a stimulus train the degree of saturation of the change in fura-2 fluorescence per stimulus is more pronounced for larger changes in bulk calcium, and this is the basis of the approach described here to detect changes in calcium influx. We assume that a single buffer, the indicator dye, with parameters as defined in Table A1, is in equilibrium with calcium.

$$K_B = \frac{[\mathrm{Ca}][\mathrm{B}]}{[\mathrm{CaB}]}. \tag{A1}$$

Consider the case in which $[\mathrm{Ca}]_i$ starts off at 0 and a single stimulus increases calcium levels by $\Delta[\mathrm{Ca}]_1$. If the cell contains an indicator (B), then after a single stimulus the fraction of indicator bound to calcium ($[\mathrm{CaB}]_1$) is given by the expression,

$$\left(\frac{[\mathrm{CaB}]_1}{[\mathrm{B}]_{\mathrm{tot}}}\right) = \left(1 + \frac{K_B}{\Delta[\mathrm{Ca}]_1}\right)^{-1}. \tag{A2}$$

Table A1. Definitions of parameters

$[\mathrm{Ca}]$	Concentration of free calcium
$[\mathrm{B}]$	Concentration of buffer not bound to calcium
$[\mathrm{B}]_{\mathrm{tot}} = [\mathrm{B}] + [\mathrm{CaB}]$	Total buffer concentration
$[\mathrm{CaB}]$	Concentration of buffer bound to calcium
K_B	Dissociation constant of buffer
$\Delta[\mathrm{Ca}]_1$	Change in [Ca] produced by one stimulus
$\Delta[\mathrm{CaB}]_1$	Change in [CaB] produced by one stimulus
$\Delta[\mathrm{CaB}]_2$	Change in [CaB] produced by two stimuli
$[\mathrm{Ca}]_R$	Resting concentration of free calcium
R_{21}	$\Delta[\mathrm{CaB}]_2/\Delta[\mathrm{CaB}]_1$
α	Fractional change in calcium concentration
β	Fractional change R_{21} in corresponding to a
$\Delta[\mathrm{Ca}]_1^* = (1+\alpha)\Delta[\mathrm{Ca}]_1$	New change in [Ca] produced by one stimulus
$R_{21}^* = (1+\beta)R_{21}$	New R_{21}

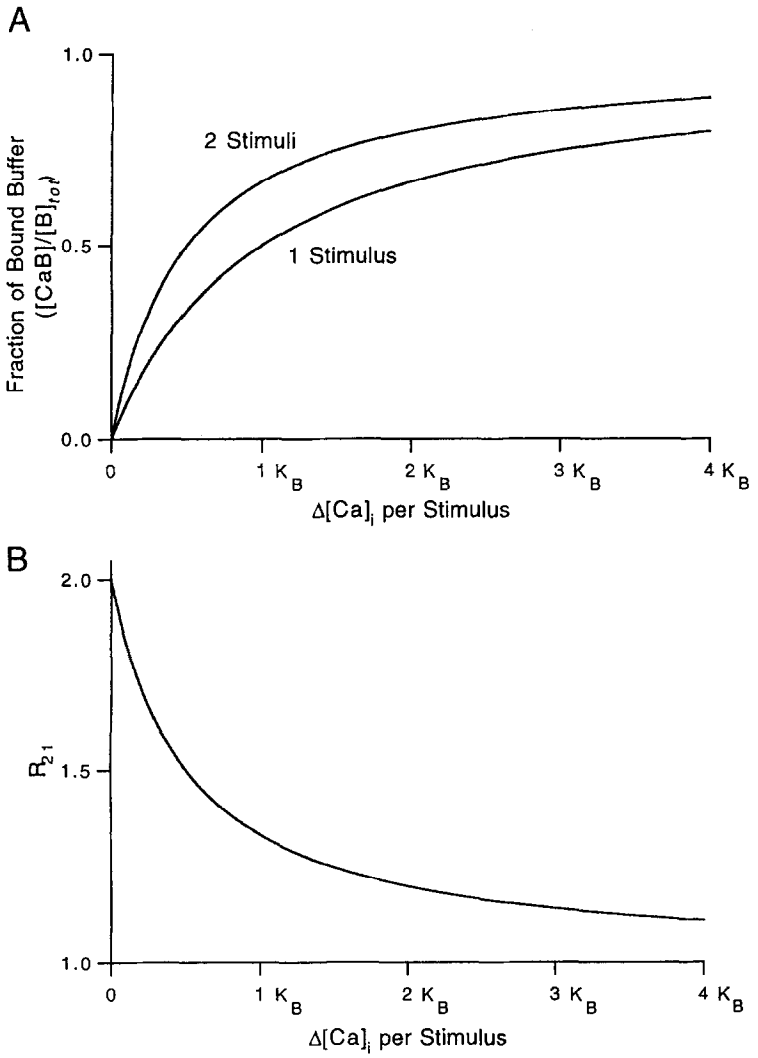

Fig. A1. Simulated changes in the fraction of buffer bound to calcium for 1 and 2 stimuli (A) and their ratio (B), calculated using Eqs (A2–A4). $\Delta[Ca]_i$ is expressed in terms of the dissociation constant of the indicator (K_B).

Similarly the calcium increase produced by 2 stimuli is given by

$$\left(\frac{[CaB]_2}{[B]_{tot}}\right) = \left(1 + \frac{K_B}{2\Delta[Ca]_1}\right)^{-1}. \quad (A3)$$

Figure A1(A) shows the fractional change of buffer bound to calcium for 1 and 2 stimuli as a function of the magnitude of the change in residual calcium, as determined from Eqs (A2) and (A3). Both $[CaB]_1$ and $[CaB]_2$ increase as the calcium change per stimulus increases, but there is appreciable saturation.

The ratio of the fraction of buffer which binds calcium for two and one stimuli is given by

$$R_{21} = \frac{[CaB]_2}{[CaB]_1} = \frac{2\left(\frac{\Delta[Ca]_1}{K_B} + 1\right)}{2\left(\frac{\Delta[Ca]_1}{K_B}\right) + 1}. \quad (A4)$$

This expression is plotted in Fig. A1(B). When a stimulus increases calcium by only a very small amount ($\Delta[Ca]_1/K_B << 1$) there is a linear relationship between the number of stimuli and the amount of calcium bound to the indicator and $R_{21} = 2$. For very large calcium changes per stimulus ($\Delta[Ca]_1/K_B >> 1$) the response of the indicator saturates and $R_{21} = 1$.

The situation is slightly more complicated than that described in Eq. (A4), because at rest the calcium concentration inside a cell is not zero, and some of the indicator is bound to calcium. If the cell has a resting calcium concentration $[Ca]_R$ then the change in concentration of indicator bound to calcium is given by,

$$\left(\frac{\Delta[CaB]_1}{[B]_{tot}}\right) = \left(1 + \frac{K_B}{\Delta[Ca]_1 + [Ca]_R}\right)^{-1} - \left(1 + \frac{K_B}{[Ca]_R}\right)^{-1} \quad (A5)$$

and for 2 stimuli is given by,

$$\left(\frac{\Delta[CaB]_2}{[B]_{tot}}\right) = \left(1 + \frac{K_B}{2\Delta[Ca]_1 + [Ca]_R}\right)^{-1} - \left(1 + \frac{K_B}{[Ca]_R}\right)^{-1} \quad (A6)$$

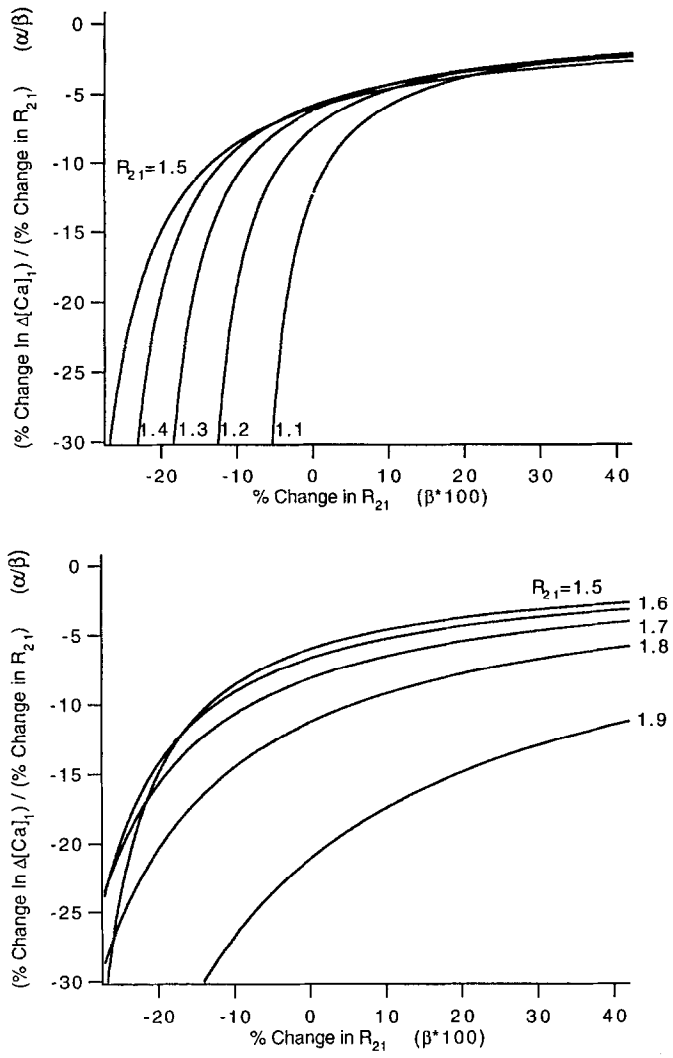

Fig. A2. Curves relating changes in R_{21} to changes in calcium influx. Traces are calculated for the indicated values of R_{21} according to Eq. (A9).

Then,

$$R_{21} = \frac{\Delta[\mathrm{CaB}]_2}{\Delta[\mathrm{CaB}]_1} = \frac{2\left(\frac{\Delta[\mathrm{Ca}]_1}{K_B} + \frac{[\mathrm{Ca}]_R}{K_B} + 1\right)}{2\left(\frac{\Delta[\mathrm{Ca}]_1}{K_B}\right) + \frac{[\mathrm{Ca}]_R}{K_B} + 1} \tag{A7}$$

and

$$\Delta[\mathrm{Ca}]_1 = \frac{([\mathrm{Ca}]_R + K_B)}{2}\left(\frac{2 - R_{21}}{R_{21} - 1}\right) \tag{A8}$$

If a manipulation of calcium influx changes R_{21} to $R^*_{21} = (1 + \beta)R_{21}$ then the fractional change in the calcium influx is given by

$$1 + \alpha = \frac{\Delta[\mathrm{Ca}]^*_1 - [\mathrm{Ca}]_1}{\Delta[\mathrm{Ca}]_1} = \left(\frac{(1+\beta)R_{21} - 2}{(1+\beta)R_{21} - 1}\right)\left(\frac{R_{21} - 1}{R_{21} - 2}\right) \tag{A9}$$

Note that this quantity is independent of both the dissociation constant of the indicator and the resting calcium concentration. Thus we can determine the fractional alteration in the calcium influx by measuring R_{21} both in control conditions and after influx has been altered. The fractional change in calcium can then be determined from Eq. (A9). This method has the major advantage that it provides a measure of changes in calcium influx which is insensitive to the number fibers activated.

As shown in Fig. (A2), the fractional change in R_{21} is smaller than the fractional change in calcium. This figure also aids in selecting the appropriate dye to detect changes in calcium concentration. Ideally the dissociation constant of the dye should be comparable to the increase in free calcium produced by a single stimulus and $1.3 < R_{21} < 1.7$. As R_{21} approaches 1 it becomes increasingly difficult to quantify calcium changes with this method, because even a relatively large change in influx corresponds to small change in R_{21}. This is particularly true for the detection of increases in calcium influx, as a single stimulus triggers sufficient calcium influx to nearly saturate the indicator. For example, if $R_{21} = 1.1$ an increase in calcium influx of about 150% corresponds to a decrease of just 5% in R_{21}; such a small change in R_{21} is difficult to detect. As R_{21} approaches 2 it is also difficult to detect changes in influx, but in this range the difficulty arises from too little saturation of the dye.

While this technique can be applied to other preparations, it

is important to establish that the assumptions made in the derivations of the equations are valid in each experimental condition. In particular, the same number of fibers must be activated by the first and second stimulation used in the determination of R_{21}. It is also assumed that the indicator dye is present in low enough concentrations that it does not significantly alter the normal calcium dynamics.

Acknowledgements—We thank J. Dittman and P. Atluri for comments on the manuscript. This work was supported by NIH NS32405, a McKnight Scholars Award, and a Klingenstein Fellowship Award in the Neurosciences to W.R. B.S. was supported by NIH training agent T32EY07110-06.

REFERENCES

Alford S., Frenguelli B. G., Schofield J.G. and Collingridge G. L. (1993) Characterization of Ca^{2+} signals induced in hippocampal CA1 neurones by the synaptic activation of NMDA receptors. *J. Physiol.* **469:** 693–716.

Chavez-Noriega L. E. and Stevens C. F. (1994) Increased transmitter release at excitatory synapses produced by direct activation of adenylate cylase in rat hippocampal slices. *J. Neurosci.* **14:** 310–317.

Chavis P., Shinozaki H., Bockaert J. and Fagni L. (1994) The metabotropic glutamate receptor types 2/3 inhibit L-type calcium channels via a pertussis toxin-sensitive G-protein in cultured cerebellar granule cells. *J. Neurosci.* **14:** 7067–7076.

Cohen M. W., Jones O. T. and Angelides K. J. (1991) Distribution of Ca^{2+} channels on frog motor nerve terminals revealed by fluorescent ω-conotoxin. *J. Neurosci.* **11:** 1032–1039.

Delaney K., Tank D. W. and Zucker R. S. (1991) Presynaptic calcium and serotonin-mediated enhancement of transmitter release at crayfish neuromuscular junction. *J. Neurosci.* **11:** 2631–2643.

Delbono O. and Stefani E. (1993) Calcium transients in single mammalian skeletal muscle fibers. *J. Physiol.* **463:** 689–707.

Eccles J. C., Ito M. and Szentagothai J. (1967) *The Cerebellum as a Neuronal Machine*. Springer-Verlag, New York.

Ellisman M. H., Deerinck T. J., Ouyang Y., Beck C. F., Tanksley S. J., Walton P. D., Airey J. A. and Sutko J. L. (1990) Identification and localization of ryanodine binding proteins in the avian central nervous system. *Neuron* **5:** 135–146.

Feher J. J. and Lipford B. G. (1985) Mechanism of action of ryanodine on cardiac sarcoplasmic reticulum. *Biochimica et Biophysica Acta* **813:** 77–86.

Feller M., Delaney K. and Tank D. (1995) Submitted.

Grynkiewicz G., Poenie M. and Tsien R. Y. (1985) A new generation of Ca^{2+} indicators with greatly improved fluorescence properties. *J. Biol. Chem.* **260:** 3440–3450.

Herrington J. and Bookman R. J. (1994) *Pulse Control V3.0: IGOR XOPs for Patch Clamp Data Acquisition*. University of Miami, Miami, FL.

Hillyard D. R., Monje V. D., Mintz I. M., Bean B. P., Nadasdi L., Ramachandran J., Miljanich G., Azimi-Zoonooz A., McIntosh J. M., Cruz L. J., Imperial J. S. and Olivera B. M. (1992) A new conus peptide ligand for mammalian presynaptic Ca2+ channels. *Neuron* **9:** 69–77.

Honore T., Davies S. N., Drejer J., Fletcher E. J., Jacobsen P., Lodge D. and Nielsen F. E. (1988) Quinoxalinediones: potent competitive non-NMDA glutamate receptor antagonists. *Science* **241:** 701–703.

Iatridou H., Foukaraki E., Kuhn M. A., Marcus E. M., Haugland R. P. and Katerinopoulos H. E. (1994) The development of a new family of intracellular calcium probes. *Cell Calcium* **15:** 190–198.

Irving A. J., Collingridge G. L. and Schofield J. G. (1992) Interactions between Ca^{2+} mobilizing mechanisms in cultured rat cerebellar granule cells. *J. Physiol.* **456:** 667–680.

Katz B. and Miledi R. (1967) The timing of calcium action during neuromuscular transmission. *J. Physiol., Lond.* **189:** 535–544.

Konnerth A., Llano I. and Armstrong C. M. (1990) Synaptic currents in cerebellar Purkinje cells. *Proc. Natn. Acad. Sci. U.S.A.* **87:** 2662–2665.

Kuwajima G., Futatsugi A., Niinobe M., Nakanishi S. and Mikoshiba K. (1992) Two types of ryanodine receptors in mouse brain: skeletal muscle type in exclusively in Purkinje cells and cardiac muscle type in various neurons. *Neuron* **9:** 1133–1142.

Llano I., Marty A., Armstrong C. M. and Konnerth A. (1991) Synaptic-and agonist-induced excitatory currents of Purkinje cells in rat cerebellar slices. *J. Physiol.* **434:** 183–213.

Llano I., DiPolo R. and Marty A. (1994) Calcium-induced calcium release in cerebellar Purkinje cells. *Neuron* **12:** 663–673.

Lytton J., Westlin M. and Hanley M. R. (1991) Thapsigargin inhibits the sarcoplasmic and endoplasmic reticulum Ca-ATPase family of calcium pumps. *J. Biol. Chem.* **266:** 17067–17071.

Mintz I. M., Adams M. E. and Bean B. P. (1992a) P-type calcium channels in rat central and peripheral neurons. *Neuron* **9:** 85–95.

Mintz I. M., Venema V. J., Swiderek K. M., Lee T. D., Bean B. P. and Adams M. E. (1992b) P-type calcium channels blocked by the spider toxin ω-Aga-IVA. *Nature* **355:** 827–829.

Mintz I. M., Sabatini B. L. and Regehr W. G. (1995) Calcium control of transmitter release at a central synapse. *Neuron* **15:** 675–688.

Neher E. and Augustine G. J. (1992) Calcium gradients and buffers in bovine chromaffin cells. *J. Physiol.* **450:** 273–301.

Palay S. L. and Chan-Palay V. (1974) Cerebellar Cortex. Springer-Verlag, New York.

Palkovits M., Magyar P. and Szentagothai J. (1971) Quantitative histological analysis of the cerebellar cortex in the cat. III. Structural organization of the molecular layer. *Brain Res.* **34:** 1–18.

Raju B., Murphy E., Levy L. A., Hall R. D. and London R. E. (1989) A fluorescent indicator for measuring cytosolic free magnesium. *Am. J. Physiol.* **256:** C540–C548.

Randall A. and Tsien R. W. (1995) Pharmacological dissection of multiple types of Ca^{2+} channel currents in rat cerebellar granule cells. *J. Neurosci.* **15:** 2995–3012.

Regehr W. G. and Atluri P. (1995) Calcium transients in cerebellar granule cell presynaptic terminals. *Biophys. J.* **68:** 2156–2170.

Regehr W. G. and Tank D. W. (1991a) Selective fura-2 loading of presynaptic terminals and nerve cell processes by local perfusion in mammalian brain slice. *J. Neurosci. Meth.* **37:** 111–119.

Regehr W. G. and Tank D. W. (1991b) The maintenance of

LTP at hippocampal mossy fiber synapses is independent of sustained presynaptic calcium. *Neuron* **7:** 451–459.

Regehr W. G. and Tank D. W. (1992) Calcium concentration dynamics produced by synaptic activation of CA1 hippocampal pyramidal cells. *J. Neurosci.* **12:** 4202–4223.

Regehr W. G., Delaney K. R. and Tank D. W. (1994) The role of presynaptic calcium in short-term enhancement at the hippocampal mossy fiber synapse. *J. Neurosci.* **14:** 523–537.

Robitaille R. and Charlton M. P. (1992) Presynaptic calcium signals and transmitter release are modulated by calcium-activated potassium channels. *J. Neurosci.* **12:** 297–305.

Rousseau E., Smith J. S. and Meissner G. (1987) Ryanodine modifies conductance and gating behavior of single calcium release channels. *Am. J. Phys.* **253:** C364–368.

Sagara Y. and Inesi G. (1991) Inhibition of the sarcoplasmic reticulum transport ATPase by thapsigargin at subnanomolar concentrations. *J. Biol. Chem.* **266:** 13503–13506.

Schweizer F. E., Betz H. and Augustine G. J. (1995) From vesicle docking to endocytosis: intermediate reactions of exocytosis. *Neuron* **14:** 689–696.

Sharp A. H., McPherson P. S., Dawson T. M., Aoki C., Campbell K. P. and Snyder S. H. (1993) Differential immunohistochmeical localization of inositol 1,4,5-trisphosphate-and ryanodine-sensitive Ca^{2+} release channels in rat brain. *J. Neurosci.* **13:** 3051–3063.

Smellie F. W., Davis C. W., Daly J. W. and Wells J. N. (1979) Alkylxanthines: inhibition of adenosine-elicited accumulation of cyclic AMP in brain slices and of brain phosphodiesterase activity. *Life Sci.* **24:** 2475–2482.

Smith S. J., Buchanan J., Osses L. R., Charlton M. P. and Augustine G. J. (1993) The spatial distribution of calcium signals in squid presynaptic terminals. *J. Physiol., Lond.* **472:** 573–593.

Takei K., Stukenbrok H., Metcalf A., Mignery G. A., Sudhof T. C., Volpe P. and De Camilli P. (1992). Ca^{2+} Stores in Purkinje Neurons: Endoplasmic reticulum subcompartments demonstrated by the heterogeneous distribution of the InsP3 receptor, Ca^{2+}-ATPase, and calsequestrin. *J. Neurosci.* **12:** 489–505.

Tank D. W., Regehr W. G. and Delaney K. R. (1995) A quantitative model of calcium dynamics that contribute to short term synaptic enhancement. *J. Neurosci.* In press.

Wu L.-G. and Saggau P. (1994a) Adenosine inhibits evoked synaptic transmission primarily by reducing presynaptic calcium influx in area CA1 of hippocampus. *Neuron* **12:** 1139–1148.

Wu L.-G. and Saggau P. (1994b) Pharmacological identification of two types of presynaptic voltage-dependent calcium channels at CA3-CA1 synapses of the hippocampus. *J. Neurosci.* **14:** 5613–5622.

Wu L.-G. and Saggau P. (1994c) Presynaptic calcium is increased during normal synaptic transmission and paired-pulse facilitation, but not in long term potentiation in area CA1 of hippocampus. *J. Neurosci.* **14:** 645–654.